Research Article
doi: 10.1590/01047760202330013343
vol(30), 2024

CERNE

Valorization of *Paulownia tomentosa* wood wastes to produce cellulose nanocrystals

Carline Andréa Welter[1], Daniel Tavares de Farias[1], Pedro Henrique Gonzalez de Cademartori[2], Cristiane de Bona da Silva[1], Cristiane Pedrazzi[1]✤

[1]Federal University of Santa Maria, Brazil
[2]Federal University of Paraná, Brazil

TECHNOLOGY OF FOREST PRODUCTS

ABSTRACT

Background: *Paulownia tomentosa* wood has chemical properties that satisfy the requirements for good raw material to obtain cellulose-based products, such as nanocellulose. Cellulose nanocrystals (CNC) are derived from naturally occurring cellulosic fibers, constituted of cellulose chains with an organizational setting that results in rigid rod-shaped crystals. This study assessed the wood wastes from *Paulownia tomentosa* Steud. as raw material for producing cellulose nanocrystals (CNC) using alkaline and delignification treatments, followed by a hydrolysis process with sulfuric acid at the 52% and 58% concentrations. The isolation of CNC from *Paulownia tomentosa* wood wastes was confirmed through different spectroscopic analyses.

Results: The suspensions of nanocrystalline cellulose CNC-52 and CNC-58 showed yields of 8.34% and 7.62%, respectively. The particle size distribution of the suspensions, determined by the AFM technique, presented an average of L = 180.01 nm and W = 20.46 nm in CNC-52 and L = 128.06 nm and W = 10.18 nm in CNC-58. Moreover, the FTIR and XRD results demonstrated that there was no difference in the structure of the crystalline network and the chemical composition between cellulose (Kiri-CB) and the CNC.

Conclusion: The results obtained from this study allowed to conclude that it is possible to employ the *Paulownia tomentosa* wood waste as a source of cellulose for extracting CNC by hydrolysis, adjusting the sulfuric acid concentration to 58% and maintaining it at 45 °C for 60 min.

Keywords: wood sawdust; nanocellulose; nanowhiskers, CNC.

HIGHLIGHTS

Investigation of wood wastes as a raw material for producing cellulose nanocrystals (CNC)
Alkaline and delignification treatments, followed by a hydrolysis process with H_2SO_4
The isolation of CNC from sawdust was confirmed through different spectroscopic analyses
The highest acid concentration used resulted in more stable and crystalline CNC

WELTER, C. A.; FARIAS, D. T.; CADEMARTORI, P. H. G.; SILVA, C. B.; PEDRAZZI, C. Valorization of *Paulownia tomentosa* wood wastes to produce cellulose nanocrystals. CERNE, v.30, e-103343, doi: 10.1590/01047760202430013343.

✤Corresponding author: cristiane.pedrazzi@ufsm.br
Received: October 11/2023 Accepted: July 5/2024

Open Access
CERNE
ISSN 0104-7760
UFLA UNIVERSIDADE FEDERAL DE LAVRAS

INTRODUCTION

The species of the *Paulownia* genus, popularly known as Kiri, are commercialized primarily for solid wood products due to their soft, light wood with straight pores and satin sheen, besides the excellent machining and finishing properties of the wood (Kalaycioglu et al., 2005; Silvestre et al., 2005). However, the forest processing industry generates waste on the order of 27,750,000 t/year in the form of coasters, trimmings, shavings, bark, and sawdust (Vieira et al., 2018). The use of sawdust to obtain fine products of high added value draws even more attention due to the environmental issues compared to oil-based synthetic materials.

Plant biomass is the primary source of biopolymer for sustainable and renewable uses in the manufacturing of chemical bioproducts, materials, and fuels (Emam et al., 2017; Vallejos et al., 2016). Biopolymers are high added value materials attractive due to their biodegradability, low density, and excellent mechanical properties (Collazo-Bigliardi et al., 2018). Nanocellulose stands out among the fine products, with promising application opportunities.

Between nanocellulose categories, the nanocrystalline cellulose is considered a valuable, sustainable nanomaterial with desirable characteristics capable of improving chemical, physical, mechanical, optical, and thermal properties when applied to films, coating, smart packaging, biomedical devices, hydrogels, wastewater treatments, and the automotive industry, among other nanoengineered applications (Curvello et al., 2019; Lasrado et al., 2020; Lopez-Polo et al., 2020).

Paulownia tomentosa wood contains 68% of holocellulose, and 62% of alfa-cellulose (Welter, 2021). Also, *Paulownia* wood has a series of properties that satisfy the requirements for good raw material to obtain cellulose-based products such as nanocellulose (Ashori and Nourbakhsh, 2009).

The utilization of *Paulownia tomentosa* wood waste for cellulose nanocrystal production via acid hydrolysis offers a promising avenue for sustainable resource management and value-added product development. By employing acid hydrolysis, the amorphous regions of cellulose within the wood waste can be selectively cleaved, yielding cellulose nanocrystals with high aspect ratios and desirable properties (Habibi, 2014). This approach not only addresses the environmental challenges associated with wood waste disposal but also creates opportunities for the development of eco-friendly materials with diverse applications.

Considering the potential of nanocellulose and embracing the principles of the circular economy, we present a comprehensive investigation into the utilization of ***Paulownia tomentosa*** Steud. wood wastes (sawdust) as a raw material for producing cellulose nanocrystals (CNC).

MATERIAL AND METHODS

Materials

This study used sawdust from 13-years-old *Paulownia tomentosa* wood were collected in a stand in Tuparendi, RS, Brazil; sodium hydroxide, 80% sodium chlorite, sodium acetate, glacial acetic acid, and 98.08% sulfuric acid, all laboratory-grade reagents.

Extraction of the cellulose from *Paulownia tomentosa* wood

The *Paulownia tomentosa* wood was initially transformed into sticks, ground in a Willey knife mill, and the sawdust with granulometry under 60 mesh was obtained and identified as Kiri-M. The cellulose fibers were obtained from the sawdust through the sequential extraction of hemicellulose and lignin from the raw material using alkaline and delignification procedures, following the methodology presented below and described by Moriana et al. (2016) and Vallejos et al. (2016).

The sawdust was initially boiled in water for 20 min at 100 °C and dried in an oven at 70 °C for 48 h. Next, the sample was submitted to the alkaline treatment with a 1.0 M NaOH agitation for 2 h at 80 °C under constant stirring and a 50 g/L ratio of sawdust for the solution. With the alkaline treatment time elapsed, the sample was washed with hot water, and the residual alkaline sawdust was delignified in an acid solution of 15 g of sodium acetate, 15 g of 80% sodium chlorite, and 100 drops of glacial acetic acid diluted in 1600 mL of distilled water, using the material-to-liquor ratio of 1:16 (m/v) for 1 h at 80 °C, under constant agitation. This procedure was repeated three times, and, at the end of each cycle, the sample was exhaustively washed with hot water to remove the excess/unreacted chemicals. The obtained cellulose sample was dried in an oven at 40 °C and identified as Kiri-CB.

Extraction of cellulose nanocrystals (CNC)

The method for obtaining the cellulose nanocrystals from the Kiri-CB sample was carried out as described in the literature (Kumar et al., 2022). Initially, experiments were performed using higher acid concentrations, as typically referenced in the literature (Kumar et al., 2014; Zheng et al., 2024). Nevertheless, it became evident that the material was prone to degradation under these conditions, necessitating a reduction in concentration to facilitate a gentler chemical reaction.

The Kiri-CB sample was hydrolyzed with sulfuric acid (H_2SO_4) diluted at the 52% and 58% concentrations, with an acid-to-cellulose ratio of 1:10 (m/v), in a water bath heated to 45 °C under vigorous mechanical agitation for 60 min. The hydrolysis was interrupted by adding cold distilled water at a volume eight times that of the initial reaction. The obtained suspension was centrifuged for 15 min at 15,000 rpm at 10 °C (CR Himac 21GII centrifuge, Hitachi) and washed with distilled water. The procedure was performed five times until the supernatant acquired a cloudy color. In sequence, the precipitate collected in the centrifugation was dialyzed in regenerated cellulose membranes (10,000 DA) for several days until the neutrality of the dialysis effluent was reached. The resulting CNC suspension was submitted to sonication at a 30% amplitude and 50 °C for 30 min in an ice bath. Part of this material was collected and sent to Zetasizer and Atomic Force Microscopy analysis. Aliquots of 5 mL were collected for determining the concentration of the nanocellulose suspensions by gravimetry through

oven drying at 40 °C, and the calculation of percent yield (m/m). The rest of the material was lyophilized (-50 °C, 0.1 mbar) to obtain dry CNC and sent to the other analyses. The cellulose nanocrystals samples obtained from the acid hydrolysis with 52% and 58% sulfuric acid were identified as CNC-52 and CNC-58, respectively.

Characterization of the CNC

Zeta potential and dynamic light scattering

The zeta potential values were assessed by determining the electrophoretic mobility using the Nano ZS Zetasizer (Malvern Instruments). The samples for zeta potential were placed in a zeta cell (cell 1070). The measurement was repeated three times for each sample, and the average was calculated.

Particle size measurements were also carried out through dynamic light scattering (DLS). Because cellulose nanocrystal has an acicular geometry, the data were represented through the conversion into spheres of equal volume, thus indicating the average diameter of the equivalent sphere.

For the zeta potential and DLS analyses, suspensions of CNC in aqueous medium at a concentration of 0.01% were used. The zeta cell has a capacity of about 1 mL, and the analyses were conducted at 25 ºC, with a spectral range of -200 to 200 mV for zeta potential and 0.1 to 10000 nm for DLS.

Atomic Force Microscopy (AFM)

Atomic force microscopy was used to verify the morphology and dimensions of isolated cellulose nanocrystals. To perform the analysis, CNC suspensions at 0.001% were homogenized in ultrasonic probe processor for 10 min at 30% amplitude, dripd into mica substrate and dried at room temperature. Several samples were analyzed, and representative micrographs were selected, and analyzed with ImageJ software (Schneider et al., 2012) to measure the length and width of at least 75 individual nanocrystals of each sample. To verify the effect of H_2SO_4 concentration on nanocrystal dimensions, this T for two independent samples (α=0.05) was applied to the observed length-to-width values using the OriginLab software.

X-Ray diffraction (XRD) analysis

The XRD patterns of the cellulose (Kiri-CB) and dry CNC were obtained using a Rigaku Diffractometer (model Miniflex® 300) operated at 30 kV and 10 mA, using a Cu Kα radiation source (λ = 1.54051 Å). The crystallinity index (CI, %) was calculated following the Segal Equation 1, commonly employed for lignocellulosic materials (El Achaby et al., 2018):

$$CI = \left(1 - \frac{I_{am}}{I_{200}}\right) \times 100 \quad (1)$$

where $I_{(200)}$ represents the intensity of the peak between 22° and 23° for the crystalline and amorphous part, and $I_{(am)}$ is the intensity of the peak between 15° and 16° and represents the amorphous part of the cellulose.

Fourier-transform infrared spectroscopy (FTIR)

The infrared spectroscopy analyses were performed in the wood waste (Kiri-M), cellulose (Kiri-CB) and CNC samples using the Shimadzu IR Prestige equipment by the direct transmittance method employing the KBr pellet (disk form) technique. The spectra were obtained in the 400 cm^{-1} to 4500 cm^{-1} range, with a sweep of 45 scans and a 2 cm^{-1} resolution.

Thermogravimetric analysis (TGA)

The thermogravimetric analysis of the Kiri-M and the powder obtained after drying the CNC-52 and CNC-58 suspensions was performed using NETZSCH TG 209F1 equipment. This technique was used to detect changes on the thermal stability of the cellulosic fiber, primarily due to the acid hydrolysis procedure. The samples were heated up to 800 °C at a heating rate of 10 °C/min and gas flow of 1 L/min.

RESULTS

Cellulose nanocrystals extraction and Zetasizer analysis

The CNC-52 and CNC-58 nanocrystalline cellulose suspensions presented yields of 8.34% and 7.62% relative to the cellulose (Kiri-CB), respectively. The size distribution of the suspension particles, determined through the DLS technique, presented an average of 171.9 ± 4.5 nm for the CNC-52 and 169.0 ± 1.2 nm for CNC-58, without a minimum statistically significant difference (Table 1).

Table 1: Yields, zeta potentials and particle sizes (through DLS) of the CNC.

Material	Yield	Zeta potential	DLS
	%	mV	d.nm
CNC-52	8.34 a	-37.80 a	171.87 a
CNC-58	7.62 a	-53.40 b	169.03 a

*Values followed by equal letters in the same column did not differ statistically ($p < 0.05$) by Tukey's test.

Atomic force microscopy (AFM)

Through measurements of 75 individual nanocrystals in AFM micrographs, the mean L of 180.01 nm verified in CNC-52 is significantly higher than the mean L of 128.06 nm verified in CNC-58. This difference was also verified for the mean W of 20.46 nm and 10.18 nm of CNC-52 and CNC-58, respectively (Figure 1).

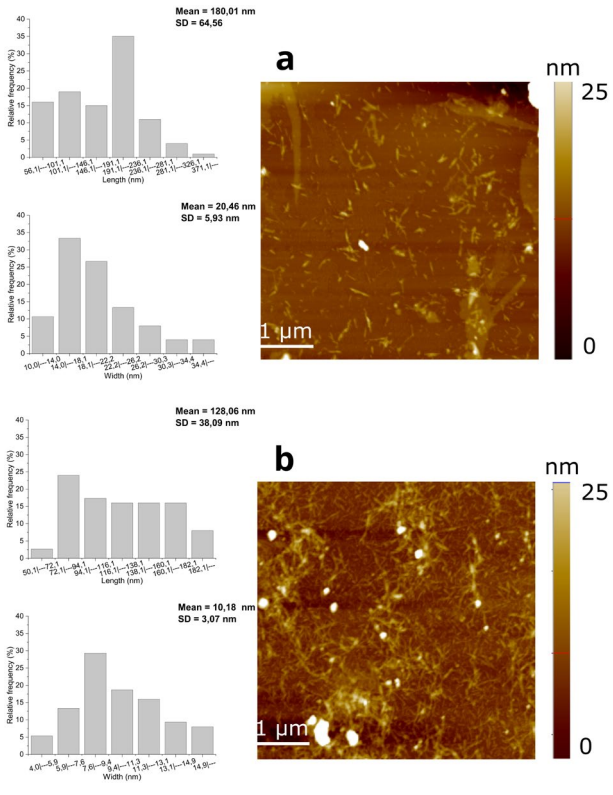

Figure 1: Atomic force microscopy of cellulose nanocrystals: **a** CNC-52 and **b** CNC-58 and their respective mean values, standard deviation and frequency distribution of width and length.

Crystallinity index

The diffraction patterns were characteristic of the crystalline structure of type I cellulose due to the presence of peaks near 2θ = 15° (plane 001), 22.5° (002), and 34° (040) (Figure 2) (Kumar et al., 2014; Morelli et al., 2012; Silvério et al., 2013).

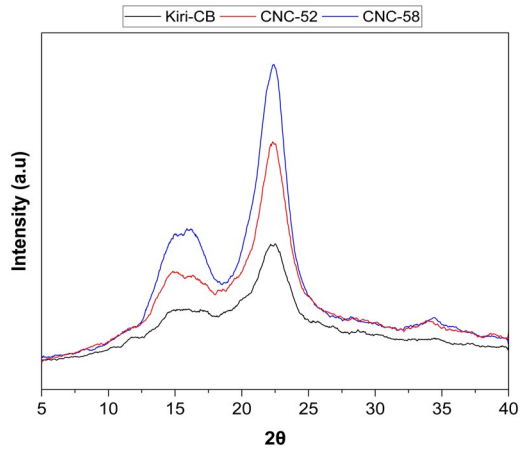

Figure 2: XRD pattern of the cellulose (Kiri-CB) and cellulose nanocrystals (CNC-52 and CNC-58).

The crystallinity index (CI) of the samples was calculated using the Segal equation, and the values of 51.8%, 57.9% and 70.7% were verified for the cellulose (Kiri-CB), CNC-52, and CNC-58, respectively (Figure 2).

Chemical features by infrared spectroscopy

To confirm the efficacy of the alkaline treatment and delignification in the removal of hemicellulose, lignin, and low molecular weight chemical components, the spectra in the infrared region were analyzed in the Kiri-M, Kiri-CB, CNC-52 and CNC-58 samples using the Fourier-transform infrared spectroscopy (FTIR) technique (Figure 3).

Thermal features of CNC

The thermal degradation behaviors of the *Paulownia tomentosa* wood waste (Kiri-M) and the CNC-52 and CNC-58 were investigated through TGA, and the results are presented in Figure 4.

The mass loss for the wood waste sample (Kiri-M) (Figure 4) indicated the occurrence of three main events: (1) the evaporation of water up to 100 °C; (2) the thermal degradation of the cellulose, with the maximum rate at the 300 °C to 325 °C range; (3) the degradation of the carbonaceous residues for temperatures over 400 °C (Ouajai and Shanks, 2005).

DISCUSSION

In the production of CNC, the sulfuric acid used in the hydrolysis selectively attacks the amorphous areas of cellulose at two levels, breaking the intramolecular hydrogen bonds within the cellulosic chains and leading to the breakage of the glycosidic bonds, so to produce shorter chains of similar morphological and crystalline structure (Shaheen and Emam, 2018). Thus, higher acid concentrations would result in lower yields, as in the present study.

The stability of the CNC produced was confirmed by monitoring the charge of particles dispersed in an aqueous solution using the analysis of the zeta potentials, which were -37.8 ± 0.36 mV for CNC-52 and -50.4 ± 0.78 mV for CNC-58. One may consider that the suspension is stable - with no tendency to flocculate - when the value (in modulus) is over 25 mV (Emam et al., 2017; Moriana et al., 2016).

CNC was also extracted from the sawdust from Egypt's carpentry and joinery processes by acid hydrolysis using sulfuric acid solution 60% by weight. The zeta potential of the nanocrystals was -39.2 mV ± 6.7 (Shaheen and Emam, 2018). Other types of biomass waste were used as a source of cellulose for CNC extraction, such as jute fiber waste (Rana et al., 2021), *Cucumis sativus* peels (Prasanna and Mitra, 2020), lemon seeds (Zhang et al., 2020), and date palm stem (Raza et al., 2022), under high concentration of sulfuric acid (> 60% by weight). The zeta potential values are between -33 mV and -41 mV, corroborating with results found in this research with kiri wood waste.

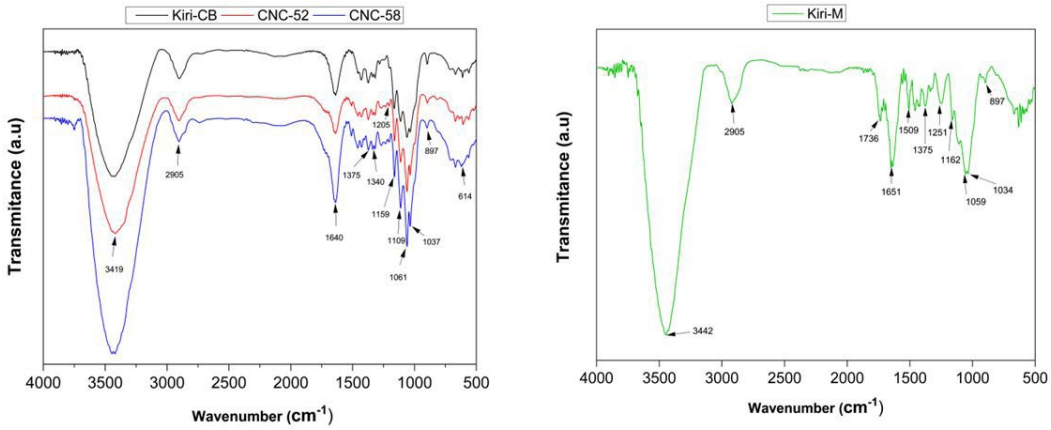

Figure 3: FTIR spectra. **A**: *Paulownia tomentosa* wood waste (Kiri-M); **B**: Cellulose (Kiri-CB) and cellulose nanocrystals (CNC-52 and CNC-58).

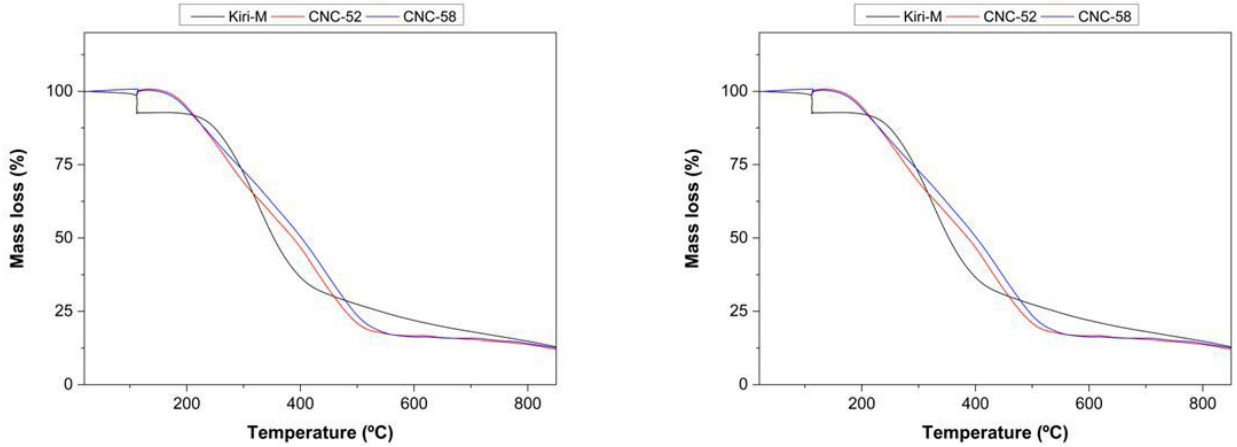

Figure 4: TGA thermograms. **A**: Mass loss (%) and **B**: mass-loss rate (%/°C) for Kiri-M, CNC-52, CNC-58.

In this research, we showed that it is possible to obtain CNC with optimal stability due to the presence of negatively charged sulfate groups chemically bonded to the surface of the CNC as the cellulose fibers are hydrolyzed to release the CNC. We also demonstrated that increasing the sulfuric acid concentration from 52% to 58% results in significantly ($p<0.05$) higher zeta potential values.

The DLS analysis is usually used to verify the size of CNC since it is easy to perform and quickly obtain the results. The DLS results expressed in Table 1 showed that the CNC extracted in the present study are within the size range observed for various types of waste, such as agave (Gallardo-Sánchez et al., 2021), jute fiber residues (Rana et al., 2021), *Cucumis sativus* peels (Prasanna and Mitra, 2020), lemon seeds (Zhang et al., 2020), and date palm stem (Raza et al., 2022), with values between 123.53 nm and 344.5 nm. The kiri wood waste used in the present study presented values of 171.87 nm for CNC-52 and 169.03 nm for CNC-58, without significant differences between treatments.

Many factors can affect the morphology and dimensions of cellulose nanocrystals, for example, the source of cellulose and acid hydrolysis conditions. The dimensions, influence their performance as a reinforcing material in polymeric matrices, and therefore, it is important to conduct the hydrolysis reaction under controlled conditions to obtain cellulose nanocrystals with adjustable size (Wang et al., 2021).

In Figure 1.a and b, it is possible to verify that the hydrolysis reaction conducted at 45°C, sulfuric acid concentration at 52% and 58%, and time of 60 min, successfully extracted CNC in the form of "rods" or "needles" regardless of the concentration of sulfuric acid used to hydrolyze *P. tomentosa* cellulose. This morphology is often described in the literature to report the typical form of cellulose nanocrystals extracted from plant cellulose (Rashid and Dutta, 2020).

The dimensions verified in the AFM micrographs for the CNC extracted from the Kiri waste confirm the DLS results expressed in Table 1. The increase in H_2SO_4 concentration from 52% to 58% resulted in significantly smaller lengths (L) and (W) widths, in which, it was observed for CNC-52 and CNC-58 W from 56.1 to 371.1 nm, and 50.1 to 182.1 nm, and W from 10.0 to 34.4 nm and 04.0 to 14.9 nm, respectively. Corroborating these results, cellulose nanocrystals (CNC)

were extracted from spruce wood cellulose using a sulfuric acid solution at 59% concentration. The length and width dimensions of the CNC were 306.7 ± 113.0 nm and 16.3 ± 3.8 nm, respectively (Kumar et al., 2022).

Based on the XRD diffractograms (Figure 2), crystallinity indices of 51.8%, 57.9%, and 70.7% were verified for Kiri-CB, CNC-52, and CNC-58, respectively. The acid hydrolysis promoted a percentage increase in the CI of 11.56% between Kiri-CB and CNC-52. The Kiri-CB sample was mainly composed of cellulose, but there was still some residual content of hemicelluloses and lignin (Figure 3). The removal of these amorphous components, which are more susceptible to acid degradation, resulted in the highest CI verified for CNC-52.

There was a considerable percentage increase of 36.22% in the crystallinity index when the acid concentration was increased from 52% to 58% to hydrolyze the Kiri-CB sample. This occurred because sulfuric acid acted as a strong depolymerization agent at a concentration of 58%, resulting in the fibers' fragmentation and releasing the most crystalline CNC.

As seen in Figure 2, characteristic peaks of type I cellulose at 2θ = 14.5 and 16.5, corresponding to halos (110) and (110), respectively, were observed in all samples. These halos referring to amorphous cellulose decreased in proportion in samples CNC-52 and CNC-58 compared to Kiri-CB, obtained after acid hydrolysis. Therefore, greater crystallinity was verified for CNC-52 and CNC-58. The peak around 22.5° at 2θ referring to the crystalline plane (200) that appears in all samples and is associated with crystalline cellulose became narrower and more prominent in samples CNC-52 and CNC-58 due to strong acid hydrolysis.

According to Figure 3, in the Kiri-M sample, the presence of spectral bands at 1251 cm^{-1} of low intensity is characteristic of the C-O ester group attributed to lignin (Xia et al., 2016), and the band at 1736 cm^{-1} is attributed to the C=0 stretching vibration of the carbonyl and acetyl groups of the hemicellulose (Oun and Rhim, 2016). Moreover, the bands at 1509 cm^{-1} and 1251 cm^{-1} (aromatic ring vibrations) were related to the presence of lignin and the form of stretching vibration of the oxygen associated with the hemicellulose, respectively (Mohamed et al., 2015).

The band present between 3500 cm^{-1} and 3200 cm^{-1} refers to the O-H stretching characteristic of cellulose, more pronounced due to the high concentration of this component in the materials (Mandal and Chakrabarty, 2011). The bands present at 897 cm^{-1} and from 1059 cm^{-1} to 1061 cm^{-1} also corresponded to the cellulose structure (Alemdar and Sain, 2008; Flauzino Neto et al., 2013), whereas the band centered at 1159 cm^{-1} to 1162 cm^{-1} was associated with the asymmetric C-O-C stretching of cellulose (Chen et al., 2016).

The band at 1640 to 1650 cm^{-1} observed in all spectra is attributed to the O-H folding vibrations of the adsorbed water (Rosa et al., 2012; Xia et al., 2016). Also, the following peaks were observed in all spectra: 1375 cm^{-1} (C-H folding); 1340 cm^{-1} (folding on the O-H bond plane); 1109 cm^{-1} (C-O-C of a glycosidic ether bond); 1060 cm^{-1} (C-O-C stretching vibration of a pyranose ring); 1034 cm^{-1} to 1037 cm^{-1} (C-O-C of a hemicellulose or lignin ether bond); 897 cm^{-1} (associated with the β-glycosidic bonds of cellulose) (Johar et al., 2012; Silvestre et al., 2005).

In the spectra for the CNC, the peak at 1205 cm^{-1} corresponded to the vibration of the S=O bond, the presence of which is related to the sulphation that occurred during the hydrolysis process with sulfuric acid (Flauzino Neto et al., 2013). Therefore, the acid hydrolysis of cellulose with sulfuric acid involves the esterification of the hydroxyl groups (Yu et al., 2021). The vital requirement in the hydrolysis process is to maintain the basic structure of the cellulose backbone (Shaheen and Emam, 2018). The spectra obtained in this study indicate that the cellulose hydrolysis process produced cellulose nanocrystals with the maintenance of the primary structure of the cellulose backbone (Figure 3).

As seen in Figure 4, a drop in the TGA curves corresponds to the peak in the DTG curves between 50 and 120 °C, indicating the evaporation of water in all samples. The onset of thermal degradation for the Kiri-M sample is observed between 226 and 290 °C and is related to the thermal decomposition of hemicelluloses, which occurs in this temperature range. This can be explained by the amorphous structure of this polysaccharide, which is more susceptible to thermal degradation than cellulose, which has a crystalline structure (Lu et al., 2014). The peak becomes wider and defined up to 500 °C due to the continuity of thermal degradation of cellulose followed by lignin.

Thermogravimetric curves CNC-52 and CNC-58 revealed two thermal events characteristic of cellulose nanocrystals hydrolyzed with sulfuric acid. The first event, observed in the range of 255 to 320 °C, marks the anticipation of the thermal degradation of cellulose and may be associated with the presence of sulfate groups that alter the chemical structure of cellulose and accelerate the thermal degradation of CNC (Travalini et al., 2016). The second thermal event, observed between 380 and 440 °C, may have occurred because of the highly crystalline structure of the CNC and the β(1–>4) glycosidic bonds, which are strong chemical bonds and require higher thermal energy to initiate thermal degradation.

CONCLUSION

This study showed that it is possible to employ the *Paulownia tomentosa* wood waste as a source of cellulose for extracting CNC by hydrolysis, adjusting the sulfuric acid concentration to 58% and maintaining it at 45 °C for 60 min. Under these acid hydrolysis conditions, the extracted CNC have widths of 4 to 40 nm, lengths between 50 and 182.1 nm, high colloidal stability in aqueous medium, and crystallinity greater than 70%. In addition, the thermal degradation study suggests that the nanocrystals produced can be used in the manufacture of new nanocomposite products whose processing temperature does not exceed 380 °C.

AUTHORSHIP CONTRIBUTION

Project Idea: C. A. W.

Funding: C. A. W., C. P.

Database: C. A. W., C. P.

Processing: C. A. W., D. T. F., C. P.

Analysis: C. A. W., D. T. F., P. H. G. C., C. B. S., C. P.

Writing: C. A. W., D. T. F., P. H. G. C., C. P.

Review: P. H. G. C., C. B. S.

REFERENCES

ALEMDAR, A.; SAIN, M. Isolation and characterization of nanofibers from agricultural residues – Wheat straw and soy hulls. Bioresource Technology, v. 99, n. 6, p. 1664–1671, 2008.

ASHORI, A.; NOURBAKHSH, A. Studies on Iranian cultivated paulownia – a potential source of fibrous raw material for paper industry. European Journal of Wood and Wood Products, v. 67, n. 3, p. 323–327, 2009.

CHEN, Y. W.; LEE, H. V.; JUAN, J. C.; et al. Production of new cellulose nanomaterial from red algae marine biomass Gelidium elegans. Carbohydrate Polymers, v. 151, p. 1210–1219, 2016.

COLLAZO-BIGLIARDI, S.; ORTEGA-TORO, R.; CHIRALT BOIX, A. Isolation and characterization of microcrystalline cellulose and cellulose nanocrystals from coffee husk and comparative study with rice husk. Carbohydrate Polymers, v. 191, p. 205–215, 2018.

CURVELLO, R.; RAGHUWANSHI, V. S.; GARNIER, G. Engineering nanocellulose hydrogels for biomedical applications. Advances in Colloid and Interface Science, v. 267, p. 47–61, 2019.

EL ACHABY, M.; EL MIRI, N.; HANNACHE, H.; et al. Production of cellulose nanocrystals from vine shoots and their use for the development of nanocomposite materials. International Journal of Biological Macromolecules, v. 117, p. 592–600, 2018.

EMAM, H. E.; EL-HAWARY, N. S.; AHMED, H. B. Green technology for durable finishing of viscose fibers via self-formation of AuNPs. International Journal of Biological Macromolecules, v. 96, p. 697–705, 2017.

FLAUZINO NETO, W. P.; SILVÉRIO, H. A.; DANTAS, N. O.; et al. Extraction and characterization of cellulose nanocrystals from agro-industrial residue – Soy hulls. Industrial Crops and Products, v. 42, p. 480–488, 2013.

GALLARDO-SÁNCHEZ, M. A.; DIAZ-VIDAL, T.; NAVARRO-HERMOSILLO, A. B.; et al. Optimization of the Obtaining of Cellulose Nanocrystals from *Agave tequilana* Weber Var. Azul Bagasse by Acid Hydrolysis. Nanomaterials, v. 11, n. 2, p. 520, 2021.

HABIBI, Y. Key advances in the chemical modification of nanocelluloses. Chemical Society Reviews, v.43, n.5, p. 1519-1542, 2014. https://doi.org/10.1039/C3CS60204D

JOHAR, N.; AHMAD, I.; DUFRESNE, A. Extraction, preparation and characterization of cellulose fibres and nanocrystals from rice husk. Industrial Crops and Products, v. 37, n. 1, p. 93–99, 2012.

KALAYCIOGLU, H.; DENIZ, I.; HIZIROGLU, S. Some of the properties of particleboard made from paulownia. Journal of Wood Science, v. 51, n. 4, p. 410–414, 2005.

KUMAR, A.; SINGH NEGI, Y.; CHOUDHARY, V.; et al. Characterization of Cellulose Nanocrystals Produced by Acid-Hydrolysis from Sugarcane Bagasse as Agro-Waste. Journal of Materials Physics and Chemistry, v. 2, n. 1, p. 1–8, 2014.

KUMAR, P.; MILLER, K.; KERMANSHAHI-POUR, A.; et al. Nanocrystalline cellulose derived from spruce wood: Influence of process parameters. International Journal of Biological Macromolecules, v. 221, p. 426–434, 2022.

LASRADO, D.; AHANKARI, S.; KAR, K. Nanocellulose-based polymer composites for energy applications—A review. Journal of Applied Polymer Science, v. 137, n. 27, p. 48959, 2020.

LOPEZ-POLO, J.; SILVA-WEISS, A.; ZAMORANO, M.; et al. Humectability and physical properties of hydroxypropyl methylcellulose coatings with liposome-cellulose nanofibers: Food application. Carbohydrate Polymers, v. 231, p. 115702, 2020.

LU, Q.; TANG, L.; WANG, S.; et al. An investigation on the characteristics of cellulose nanocrystals from *Pennisetum sinese*. Biomass and Bioenergy, v. 70, p. 267–272, 2014.

MANDAL, A.; CHAKRABARTY, D. Isolation of nanocellulose from waste sugarcane bagasse (SCB) and its characterization. Carbohydrate Polymers, v. 86, n. 3, p. 1291–1299, 2011.

MOHAMED, M. A.; SALLEH, W. N. W.; JAAFAR, J.; et al. Physicochemical properties of "green" nanocrystalline cellulose isolated from recycled newspaper. RSC Advances, v. 5, n. 38, p. 29842–29849, 2015.

MORELLI, C. L.; MARCONCINI, J. M.; PEREIRA, F. V.; et al. Extraction and characterization of cellulose nanowhiskers from balsa wood. Macromolecular Symposia, vol. 319, n.1, pp. 191-195. 2012. DOI: 10.1002/masy.201100158

MORIANA, R.; VILAPLANA, F.; EK, M. Cellulose Nanocrystals from Forest Residues as Reinforcing Agents for Composites: A Study from Macro- to Nano-Dimensions. Carbohydrate Polymers, v. 139, p. 139–149, 2016.

OUAJAI, S.; SHANKS, R. A. Composition, structure and thermal degradation of hemp cellulose after chemical treatments. Polymer Degradation and Stability, v. 89, n. 2, p. 327–335, 2005.

OUN, A. A.; RHIM, J.-W. Isolation of cellulose nanocrystals from grain straws and their use for the preparation of carboxymethyl cellulose-based nanocomposite films. Carbohydrate Polymers, v. 150, p. 187–200, 2016.

PRASANNA, N.; MITRA, J. Isolation and characterization of cellulose nanocrystals from *Cucumis sativus* peels. Carbohydrate Polymers, v. 247, p. 116706, 2020.

RANA, A. K.; FROLLINI, E.; THAKUR, V. K. Cellulose nanocrystals: Pretreatments, preparation strategies, and surface functionalization. International Journal of Biological Macromolecules, v. 182, p. 1554–1581. 2021.

RASHID, S.; DUTTA, H. Characterization of nanocellulose extracted from short, medium and long grain rice husks. Industrial Crops and Products, v. 154, p. 112627, 15. 2020.

RAZA, M.; ABU-JDAYIL, B.; BANAT, F.; et al. Isolation and Characterization of Cellulose Nanocrystals from Date Palm Waste. ACS Omega, v. 7, n. 29, p. 25366–25379, 2022. https://doi.org/10.1021/acsomega.2c02333

ROSA, S. M. L.; REHMAN, N.; DE MIRANDA, M. I. G.; et al. Chlorine-free extraction of cellulose from rice husk and whisker isolation. Carbohydrate Polymers, v. 87, n. 2, p. 1131–1138, 2012.

SCHNEIDER, C. A., RASBAND, W. S., ELICEIRI, K. W. NIH Image to ImageJ: 25 years of image analysis. Nature Methods, v. 9, n. 7, p. 671–675, 2012. doi:10.1038/nmeth.2089

SHAHEEN, Th. I.; EMAM, H. E. Sono-chemical synthesis of cellulose nanocrystals from wood sawdust using Acid hydrolysis. International Journal of Biological Macromolecules, v. 107, p. 1599–1606, 2018.

SILVÉRIO, H. A.; FLAUZINO NETO, W. P.; DANTAS, N. O.; et al. Extraction and characterization of cellulose nanocrystals from corncob for application as reinforcing agent in nanocomposites. Industrial Crops and Products, v. 44, p. 427–436, 2013.

SILVESTRE, A. J. D.; EVTUGUIN, D. V.; MENDES SOUSA, A. P.; et al. Lignans from a hybrid *Paulownia* wood. Biochemical Systematics and Ecology, v. 33, n. 12, p. 1298–1302, 2005.

TRAVALINI, A. P.; PRESTES, E.; PINHEIRO, L. A.; et al. Nanocelulose de elevada cristalinidade extraída da fibra do bagaço de mandioca. O PAPEL, v. 77, n. 1, 2016.

VALLEJOS, M. E.; FELISSIA, F. E.; AREA, M. C.; et al. Nanofibrillated cellulose (CNF) from *eucalyptus* sawdust as a dry strength agent of unrefined *eucalyptus* handsheets. Carbohydrate Polymers, v. 139, p. 99–105, 2016.

VIEIRA, A. T. D. O.; NASCIMENTO, A. M. D.; ANDRADE, A. M. D.; et al. Propriedades termoquímicas de briquetes produzidos com finos de carvão vegetal e resíduos de Pinus spp. Scientia Forestalis, v. 46, n. 119, 2018.

WANG, H.; DU, H.; LIU, K.; et al. Sustainable preparation of bifunctional cellulose nanocrystals via mixed H2SO4/formic acid hydrolysis. Carbohydrate Polymers, v. 266, p. 118107, 2021.

WELTER, C. A. Bioprodutos obtidos da madeira de *Paulownia tomentosa* Steud. 2021. 89 p. PhD thesis Universidade Federal de Santa Maria, Santa Maria.

XIA, G.; WAN, J.; ZHANG, J.; et al. Cellulose-based films prepared directly from waste newspapers via an ionic liquid. Carbohydrate Polymers, v. 151, p. 223–229, 2016.

YU, S.; SUN, J.; SHI, Y.; et al. Nanocellulose from various biomass wastes: Its preparation and potential usages towards the high value-added products. Environmental Science and Ecotechnology, v. 5, p. 100077, 2021.

ZHANG, H.; CHEN, Y.; WANG, S.; et al. Extraction and comparison of cellulose nanocrystals from lemon (*Citrus limon*) seeds using sulfuric acid hydrolysis and oxidation methods. Carbohydrate Polymers, v. 238, p. 116180, 2020.

ZHENG, Y.; WANG, Z.; HUANG, Y.; et al. Extraction and preparation of cellulose nanocrystal from Brewer's spent grain and application in pickering emulsions. Bioactive Carbohydrates and Dietary Fibre, v. 31, 2024. https://doi.org/10.1016/j.bcdf.2024.100418.